J. Phys.: Condens. Matter **20** (2008) 494201 (6pp) doi:10.1088/0953-8984/20/49/494201

# Structure of the repulsive gel/glass in suspensions of charged colloidal platelets

**M C D Mourad, D V Byelov, A V Petukhov and H N W Lekkerkerker**

Van't Hoff Laboratory for Physical and Colloid Chemistry, Utrecht University, PO Box 80.051, 3508 TB Utrecht, The Netherlands

Received 24 October 2008
Published 12 November 2008
Online at stacks.iop.org/JPhysCM/20/494201

**Abstract**

Rheological, optical and structural properties of colloidal suspensions of charge-stabilized gibbsite platelets across the sol–gel transition region are investigated. In this work we focus on samples with a low salt content ($10^{-4}$ M). While at a gibbsite concentration of 300 g $l^{-1}$, a nematic–columnar phase separation is observed, an arrested state with a nematic signature and highly elastic response has been observed for a concentration of 400 g $l^{-1}$. A temporal evolution of the structure of the arrested state, which leads to stronger interparticle correlations, has been observed on a timescale of 20 months. The results suggest that the arrested state develops into a glass with a columnar nematic structure.

(Some figures in this article are in colour only in the electronic version)

## 1. Introduction

Colloidal suspensions display intriguing phase transitions between gas, liquid, solid and liquid-crystalline phases. The spontaneous self-organized structures on sub-micrometre scales in colloidal suspensions are of potential technological interest. For example, three-dimensional arrangements of spheres in colloidal crystals might serve as photonic materials intended to manipulate light. Colloidal particles with non-spherical shapes (such as rods and plates) are of particular interest because of their ability to form liquid crystals. Nematic liquid crystals possess orientational order; smectic and columnar liquid crystals additionally exhibit positional order (in one and two dimensions respectively).The phase separation in suspensions of anisometric colloidal particles into an isotropic and a nematic phase was addressed theoretically by Lars Onsager [1] in the 1940s. He demonstrated that the thermodynamic stability of the nematic phase can be explained on a purely entropic basis by considering the competition between orientational entropy (favouring the isotropic state) and the entropy of the excluded volume (which favours the nematic state). As the latter becomes more important at higher concentrations, a first-order transition from an isotropic to a nematic phase may occur if the concentration of rods or plates is sufficiently high. Thus, even hard rods or plates may form a nematic phase. Evidence that a system of hard rods can form a thermodynamically stable smectic phase [2] and a system of hard platelets can form a thermodynamically stable columnar phase [3] was provided by computer simulations in the 1980s and 1990s.

Phase transitions in colloidal suspensions are frequently arrested by the intervention of long-lived metastable and non-equilibrium states such as gels and glasses. Colloidal suspensions are slow to reach equilibrium (if ever) from these metastable and non-equilibrium states.

This feature is particularly pronounced in aqueous suspensions of clay platelets. Due to their high aspect ratio, typically ranging between 25 and 1000, swelling clay minerals should very likely form liquid-crystalline phases. Isotropic-nematic phase equilibrium was observed by Langmuir [4] as early as 1938 in suspensions of natural hectorite. These observations provided, in part, the experimental stimulus for the theory put forward by Onsager [1]. However, it took more than half a century before further experimental evidence for liquid crystal phase equilibria in suspensions of plate-like particles was obtained [5–12].

The structure of the gel state in suspensions of charged clay platelets has been debated for a long time with two conflicting views. On the one hand, it has been suggested that the formation of a three-dimensional network is governed by electrostatic attraction of oppositely charged crystal faces [13], the so-called house of cards model [14]. On the other hand, it has been argued that the gel properties of clay suspensions should be directly related to repulsive forces caused by

 

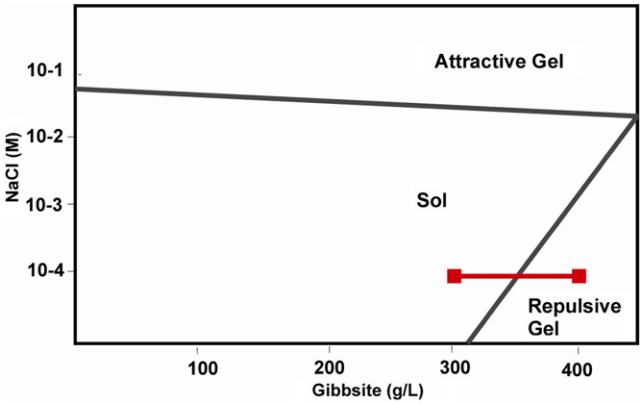


**Figure 1.** Schematic sol–gel diagram of charged colloidal gibbsite platelets in water. The sol–gel transition studied here is indicated.

interacting electric double layers [15]. By variation of the ionic strength, the balance between attractive and repulsive interactions can be tuned, leading to a sol region wedged between an attractive gel and a repulsive gel/glass. Such a rheological phase diagram has been observed for a variety of natural and synthetic clays [12, 16–19] and thus appears to be generic. A theoretical discussion has been given in [20].

We study the competition between liquid crystal formation and gelation in suspensions of charged gibbsite platelets. Gibbsite, which may be considered as a model clay particle, is intrinsically simpler because the different crystal faces at neutral pH have the same charge. Nevertheless, gibbsite has the same generic rheological phase diagram (see figure 1) as discussed above for natural and synthetic clays. An important quantitative difference is that whereas for clays the tip of the sol nose is situated at a clay concentration of 1–2 wt% and a salt concentration of $10^{-3}$–$10^{-4}$ M [12, 16–19], for gibbsite it is located at a concentration of 40–50 wt% and a salt concentration of $5 \times 10^{-2}$ M [21, 22].

Here we focus on the sol–gel transition at low salt strength (see figure 1), where repulsion is dominant. The static structure of the suspensions both in the sol and the gel region are examined by optical techniques and small-angle x-ray scattering (SAXS). In the sol region we find an isotropic (I), nematic (N) and columnar (C) phase. In the gel region a high density nematic glass is found. Examination of the ageing behaviour of this state revealed that, over years, positional order increases giving rise to an arrested columnar nematic phase [23].

## 2. Experimental details

### *2.1. Preparation*

Colloidal gibbsite platelets were grown in a two step procedure in acidic aqueous solution [24]. In the first step, hydrochloric acid (HCl 0.09 M, 37%, Merck), aluminium sec-butoxide (0.08 M, 95%, Fluka Chemika) and 0.08 M aluminium isopropoxide (98+%, Acros Organics) were dissolved in demineralized water (15 l, equally divided over three Erlenmeyer flasks). This mixture is mechanically stirred for 10 days and subsequently heated in a glass reaction vessel in a water bath at 85 °C for 72 h. Next, the colloidal dispersions were centrifuged at 1200 g (overnight, 15–20 h) in order to remove the smallest particles.

In the second step the two systems of gibbsite particles that were measured by electron microscopy to be smallest were redispersed in aqueous solution (1.5 l) of hydrochloric acid, aluminium sec-butoxide and aluminium isopropoxide (concentrations equal as described above) and heated at 85 °C for 72 h in order to perform a seeded growth. The mixture is cooled down to room temperature and centrifuged again (1200 g, overnight, 15–20 h). Finally the dispersions are added together and dialyzed against demineralized water in tubes of regenerated cellulose (Visking, MWCO 12 000–14 000) until the conductivity drops to 20 $\mu$S cm$^{-1}$. Finally aluminium chlorohydrate (0.6 g per gram gibbsite particles, Locron P, Hoechst AG, Germany) was added to the suspension to hydrolyse and form $Al_{13}$ Keggin ions ($[Al_{13}O_4(OH)_{24}(H_2O)_{12}]^{7+}$) and thereby increase the stability of the gibbsite platelets [25].

### *2.2. Particle characterization*

The resulting suspension was analysed for solid content and inspected with transmission electron microscopy (TEM). From the micrographs (see figure 2) the surface area of over 200 individual hexagonal particles was measured and transformed into an equivalent spherical diameter (ESD). Moreover the polydispersity was determined as the standard deviation in the average ESD ($\sigma_{ESD}$). The yield of the entire synthesis was determined to be 58 g (dry particle weight) with ESD = 205 nm ($\sigma_{ESD}$ = 47 nm).

### *2.3. Sample preparation and naked eye observations*

Concentrated gibbsite dispersions were prepared and set at fixed ionic strength by centrifugation and redispersion in water with NaCl added. Samples for visual observation were put in large capillaries (1.0 mm × 10.0 mm cross section, Vitrotubes, VitroCom Inc.) that were flame sealed. Visual inspection was performed on a regular basis. For this, a home-built polarization setup was used, consisting of two crossed polarizing filters that could be illuminated by a 150 W lamp in combination with a condenser lens and a ground glass diffuser for homogeneous illumination.

For x-ray experiments, samples were transferred into round Mark tubes (quartz, 2 mm diameter and about 10 $\mu$m wall thickness, W Müller, Berlin, Germany).

### *2.4. Rheological measurements*

Oscillatory experiments in the frequency range of 0.01–100 Hz were performed on gibbsite suspensions using a Physica Anton Paar (MCR-300) controlled stress rheometer operating at a strain amplitude of 0.01. It was verified that at this strain amplitude the system was in the linear viscoelastic regime at all frequencies. A cone-plate measuring geometry was used, having a diameter of 50 mm and a cone angle of 1°. The plate was kept at 20 °C by a connection with a thermostatic water

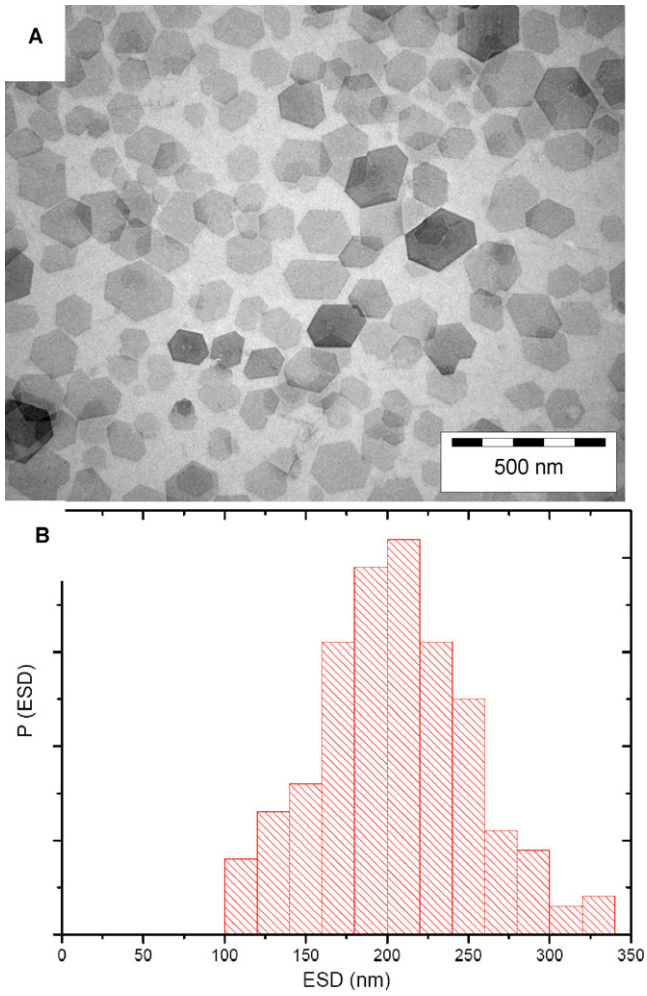


**Figure 2.** (a) Transmission electron micrograph of colloidal gibbsite platelets. (b) Histogram of the equivalent spherical diameter (ESD) of the platelet surface as determined from transmission micrographs.

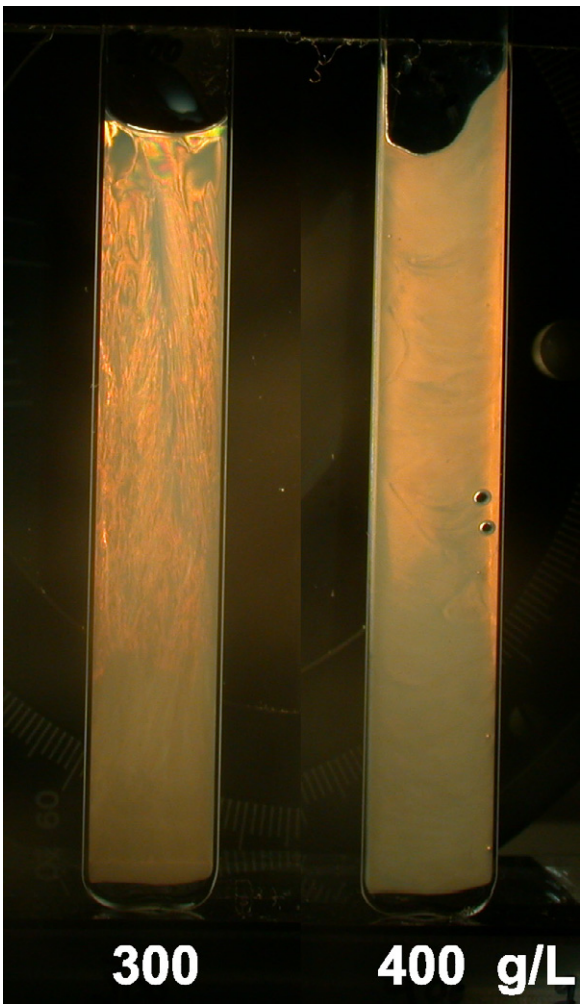


**Figure 3.** Samples of gibbsite in water with $10^{-4}$ M NaCl added, one month after homogenization as observed in between crossed polarizers.

bath. All measurements were initiated by a pre-shear (100 s at a shear rate of 500 $s^{-1}$). From the measurements the frequency dependent storage ($G'$) and loss modulus ($G''$) components of complex shear modulus $G^* = G' + iG''$ [26] were determined.

### *2.5. Small-angle x-ray scattering*

X-ray studies were performed at the Dutch–Belgian beamline BM-26 DUBBLE of the European synchrotron radiation facility (ESRF) in Grenoble, France in September 2006 with 1-month-old samples and in April 2008 using the same set of samples (20 months after preparation). We used our recently developed microradian x-ray diffraction setup similar to the one described in the literature [27]. In brief, the x-ray beam was focused by a set of compound refractive lenses (CRL) [28] at the phosphor screen of the CCD (charge-coupled device) x-ray detector (Photonic Science, $4008 \times 2671$ pixels of 22 $\mu m^2$). Any focusing of the beam before the experimental hutch was avoided to achieve maximum transverse coherence length of the beam [27]. The capillaries were placed just after the CRLs at a distance of about 8 m from the detector. This setup allows us to achieve angular resolution of the order of 5–7 $\mu$rad. The x-ray photon energies of 13 keV (wavelength $\lambda = 0.095$ nm) and 15 keV ($\lambda = 0.0825$ nm) were used in 2006 and 2008, respectively. The beam diameter in the sample was about 0.5 mm.

## 3. Results

### *3.1. Naked eye observations*

The samples already displayed remarkable differences when placed in between crossed polarizers within 24 h after homogenization. The sample at $10^{-4}$ M NaCl and 300 g $l^{-1}$ had a well-shaped meniscus at the suspension–air interface and displayed strong birefringence (figure 3). Throughout the cell vertical textures became visible. After one month the vertical patterns were still observable, but overall the appearance of the sample slightly changed. In general birefringence seemed to have increased. In particular, the region just below the meniscus showed signs of structural development during these weeks. The wetting corners of the meniscus revealed the first signs of an isotropic–nematic interface. Moreover the

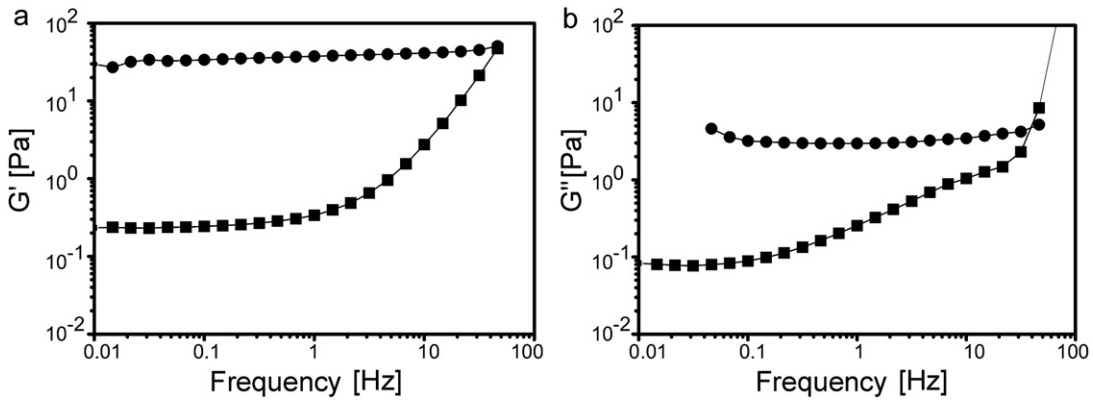


**Figure 4.** Dynamic moduli of aqueous gibbsite suspensions with $10^{-4}$ M NaCl at particle concentration of 300 g $l^{-1}$ (squares) and 400 g $l^{-1}$ (circles). In (a) the storage modulus, $G'$, is depicted while (b) displays the loss modulus, $G''$.

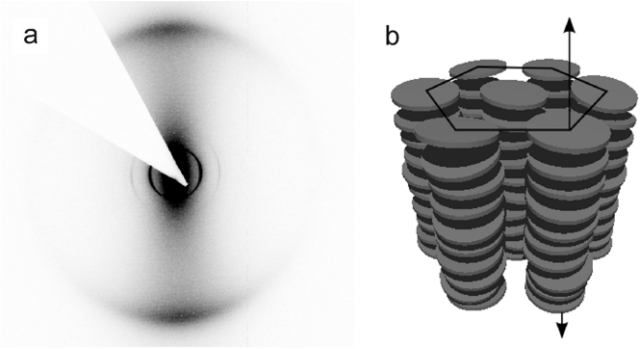


**Figure 5.** (A) An example of the x-ray diffraction pattern from the columnar phase of charged gibbsite suspension at 300 g $l^{-1}$ measured one month after preparation. Panel (B) presents a sketch of the columnar phase structure.

upper part of the nematic phase appeared darker, presumably through sample cell wall anchoring induced reorientation processes of the nematic domains. At the very bottom of the tube iridescence in the form of small Bragg reflecting spots appeared, providing evidence for the nucleation of a hexagonal columnar phase. In contrast, the sample at higher particle concentration, 400 g $l^{-1}$, displayed a perturbed meniscus right after filling due to the high viscosity which did not allow relaxation even after one month. The suspension was birefringent, although its appearance is paler than the tube at lower particle concentration. The vertical patterns, typical for the nematic phase, were absent and instead the suspension had a cloudy texture. Moreover, no signs of structural reordering could be observed by the naked eye. Both the pattern as well as the closed-in air bubbles remained unchanged during this period.

### *3.2. Rheological measurements*

The dynamic moduli were measured as a function of the oscillation frequency. While for both dispersions the storage modulus exceeds the loss modulus, some clear differences between the sample at 300 and 400 g $l^{-1}$ could be observed. In the first place the elasticity and viscosity were comparable and increased with frequency for the sample at 300 g $l^{-1}$. In contrast, for the more concentrated system (400 g $l^{-1}$) the storage modulus was approximately one order of magnitude larger than the loss modulus and both were independent of frequency. Finally the sample at higher particle concentration showed a storage modulus well above 1 Pa (figure 4). We therefore conclude that the sample at 300 g $l^{-1}$ is a sol and the sample at 400 g $l^{-1}$ can be classified as a gel [29, 30].

### *3.3. X-ray observations*

Figure 5(a) presents a typical example of a microradian x-ray diffraction pattern obtained in a 1-month-old capillary containing a suspension with a gibbsite mass fraction of 300 g $l^{-1}$ and ionic strength of $10^{-4}$ M. This suspension is in the sol region. The measurement is taken in the lower part of the capillary at a height 5 mm above the bottom and 34 mm below the top of the suspension. At small angles we observe strong sharp ring-like reflections with $q = 0.026$ and 0.0445 $nm^{-1}$. Closer inspection of the data reveals also weaker but sharp rings at $q = 0.051$ and 0.068 $nm^{-1}$. These $q$-values are related to each other as $1{:}\sqrt{3}{:}\sqrt{4}{:}\sqrt{7}$, unambiguously confirming that they originate from the (100), (110), (200) and (210) Bragg reflections of the columnar structure sketched in figure 5(b). In addition, the two broader reflections at larger $q$ (0.142 $nm^{-1}$) correspond to the (001) intracolumnar scattering and arise from the (liquid-like) ordering of the platelets within the columns.

A distinctly different pattern can be seen in the sample with the higher particle concentration (400 g $l^{-1}$), which falls into the gel region. In figure 6(a) no clear signature of the hexagonal columnar phase can be seen at small $q$. Yet, one can observe a broad and weak peak at a $q$ value of about 0.03 $nm^{-1}$. This peak suggests that there are at least some side-to-side positional correlations between the particles on a scale comparable to the particle diameter. Furthermore, one can still see a strong anisotropy in the pattern, which suggests the presence of a long-range (on distances larger than the beam size) nematic-like orientational order in the gel. This is consistent with the observed strong birefringence of this system (see figure 3). Similar to figure 5(a), at larger $q$ (here

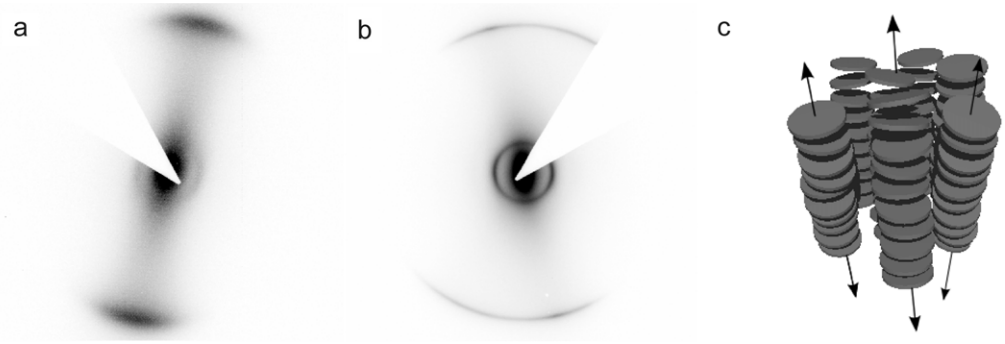


**Figure 6.** Typical x-ray diffraction patterns from the repulsive gel phase of charged gibbsite suspension at 400 g $l^{-1}$ one month (A) and 20 months (B) after sample preparation. Panel (C) presents a sketch of the columnar nematic structure.

at 0.151 $nm^{-1}$) there is also a peak corresponding to a typical face-to-face distance between the platelets of 42 nm.

These features developed in the course of time. A pattern measured at the same height in exactly the same capillary in an experiment 20 months after sample preparation is presented in figure 6(b). Both the peaks at small $q$ (0.030 $nm^{-1}$) and large $q$ (0.151 $nm^{-1}$) have significantly sharpened in comparison to that in figure 6(a). This suggests that both face-to-face and side-to-side correlations between the particles become much more pronounced. Surprisingly, the large-$q$ peak has even become sharper than the 001 peak in the columnar phase measured in 2006 (figure 5(a)) as well as in 2008 (not shown). One can clearly see that although the structure is arrested, some slow dynamics still has been present. The patterns in figure 6(a) and, in particular in figure 6(b), bear great similarity to the patterns expected for the nematic columnar ($N_c$) structure [23] sketched in figure 6(c).

## 4. Discussion

Here we have presented experimental results on the sol–gel transition for charged colloidal platelets at low ionic strength. Upon increase of the particle concentration, these systems appeared no longer to be able to form the colloidal liquid crystals, which are expected as the equilibrium phases. Naked eye observations indicated that a strongly birefringent gel has been formed that is no longer able to macroscopically phase separate to form a nematic and columnar phase as is observed for lower particle concentrations. Instead, a homogeneous gel was formed that seemed to be strong enough not to be impaired by sedimentation effects. The characteristic iridescence that usually indicates the presence of a hexagonal columnar ordering in these systems was absent. Rheological experiments by means of the measurement of the dynamic moduli support the presence of such a sol–gel transition [29, 30]. Variation of the shear frequency in the viscoelastic regime showed that the increase in particle concentration turned the storage and loss moduli from frequency dependent into frequency independent. Moreover, the magnitude of the storage modulus jumped to much larger value than that of the loss modulus, ending up well above 10 Pa.

The structural change at the sol–gel transition was investigated by SAXS. We compared x-ray scattering patterns of a columnar phase formed at the bottom of samples with overall concentration within the suspension just below the gelation concentration of a sample that does form a gel. In contrast to the columnar phase, which displays sharp ring-like hexagonal columnar 100, 110, 200 and 210 reflections, in this $q$-range the gel sample exhibits a single peak, which is a much broader and weaker peak. The position of this peak is very close, but at slightly larger $q$-value than the 100 reflection of the columnar phase. This supports the hypothesis that this gel is a kinetically arrested state of a system with the tendency to form columnar structures.

X-ray measurements on a two-year-old gel clearly indicate a further structure development. Both face-to-face as well as the side-to-side correlations between the platelets become much more pronounced. The pattern resembles that of a nematic columnar liquid crystal. In this phase the plate-like particles form stacks that in turn display nematic ordering [23]. From SAXS it can be seen that the gel-structure observed for aqueous gibbsite has developed towards a system in which such stacks have been formed.

Earlier work on gels of charged platelets has suggested that the static structure forms a Wigner glass (a glassy system in which the jamming is governed over relatively long distances by repulsive interactions) [17, 18, 20, 31]. While the results presented here are consistent with the notion of a Wigner glass, they reveal a much more detailed picture of the arrested state. To summarise, the arrested state appears to be due to the jamming of oriented columns of plate-like particles, leading to a columnar nematic glass.

## 5. Conclusion

At low ionic strength, aqueous suspensions of plate-like colloidal gibbsite particles exhibit a sol–gel transition upon increasing the gibbsite concentration. In the sol region, isotropic, nematic and hexagonal columnar are found. At higher concentration (400 g $l^{-1}$), the system ends up in an arrested state, as evidenced by a sharp increase of the elastic modulus. The system is no longer able to phase separate. SAXS measurements indicate that the structure is that of a columnar nematic phase, which is kinetically arrested.

## Acknowledgments

The Dutch Organization for Scientific Research (NWO) is thanked for the financial support of MCDM and for granting us the beamtime at the DUBBLE beamline. The authors are grateful to Kristina Kvashnina, Esther van den Pol, Anatoly Snigirev and Dirk Detollenaere for their help with the synchrotron measurements and to Annemieke ten Brinke for her expert advice and assistance in the rheological measurements.

## References

[1] Onsager L 1949 *Ann. New York Acad. Sci.* **51** 627–59
[2] Frenkel D, Lekkerkerker H N W and Stroobants A 1988 *Nature* **332** 822–3
[3] Veerman J A C and Frenkel D 1992 *Phys. Rev.* A **45** 5632–48
[4] Langmuir I 1938 *J. Chem. Phys.* **6** 873–96
[5] Brown A B D, Clarke S M and Rennie A R 1998 *Langmuir* **14** 3129–32
[6] van der Kooij F M and Lekkerkerker H N W 1998 *J. Phys. Chem.* B **102** 7829–32
[7] van der Kooij F M, Kassapidou K and Lekkerkerker H N W 2000 *Nature* **406** 868–71
[8] Liu S, Zhang J, Wang N, Liu W, Zhang C and Sun D 2003 *Chem. Mater.* **15** 3240–1
[9] van der Beek D and Lekkerkerker H N W 2003 *Europhys. Lett.* **61** 702–7
[10] van der Beek D and Lekkerkerker H N W 2004 *Langmuir* **20** 8582–6
[11] Fossum J O, Gudding E, Fonseca D d M, Meheust Y, DiMasi E, Gog T and Venkataraman C 2005 *Energy* **30** 873
[12] Michot L J, Bihannic I, Maddi S, Funari S S, Baravian C, Levitz P and Davidson P 2006 *Proc. Natl Acad. Sci.* **103** 16101–4
[13] Schofield R K and Samson H R 1954 *Discuss. Faraday Soc.* **18** 135
[14] van Olphen H 1963 *An Introduction to Clay Colloid Chemistry* (New York: Interscience) pp 93–5
[15] Norrish K 1954 *Discuss. Faraday Soc.* **18** 120
[16] Abend S and Lagaly G 2000 *Appl. Clay Sci.* **16** 201
[17] Levitz P, Lécolier E, Mourchid A, Delville A and Lyonnard S 2000 *Europhys. Lett.* **49** 672–7
[18] Shalkevich A, Stradner A, Bhat S K, Muller F and Schurtenberger P 2007 *Langmuir* **23** 3570–80
[19] Michot L J, Bihannic I, Maddi S, Baravian C, Levitz P and Davidson P 2008 *Langmuir* **24** 3127–39
[20] Tanaka H, Meunier J and Bonn D 2004 *Phys. Rev.* E **69** 031404
[21] Mourad M C D, Wijnhoven J E G J, van't Zand D D, van der Beek D and Lekkerkerker H N W 2006 *Phil. Trans. R. Soc.* A **364** 2807–16
[22] Mourad M C D *et al* 2008 in preparation
[23] Laschat S, Baro A, Steinke N, Giesselmann F, Hägele C, Scalia G, Judele R, Kapatsina E, Sauer S, Schreivogel A and Tosoni M 2007 *Angew. Chem. Int. Edn* **46** 4832–87
[24] Wijnhoven J E G J 2005 *J. Colloid Interface Sci.* **292** 403
[25] Hernandez J 1998 *Thèse de Doctorat de l'Université Pierre et Marie Curie* Université Pierre et Marie Curie, Paris, France
[26] Goodwin J W and Hughes R W 2000 *Rheology for Chemists. An Introduction* (Cambridge: Royal Society of Chemistry)
[27] Petukhov A V, Thijssen J H J, 't Hart D C, Imhof A, van Blaaderen A, Dolbnya I P, Snigirev A, Moussaid A and Snigireva I 2006 *J. Appl. Crystallogr.* **39** 137–144
[28] Snigirev A, Kohn V, Snigireva I and Lengeler B 1996 *Nature* **384** 49
[29] Winter H H and Morganelli P F C 1988 *Macromolecules* **21** 532–5
[30] Almdal K, Dyre J, Hvidt S and Kramer O 1993 *Polym. Gels Networks* **1** 5–17
[31] Bonn D, Tanaka H, Wegdam G, Kellay H and Meunier J 1999 *Europhys. Lett.* **45** 52